

# Combinatorial Optimization for Electrode Labeling of EEG Caps

Mickaël Péchaud<sup>1</sup>, Renaud Keriven<sup>1</sup>, Théo Papadopoulo<sup>1</sup>, Jean-Michel Badier<sup>2</sup>

<sup>1</sup> Odyssee Lab,  
École Normale Supérieure, École des Ponts, INRIA.  
45, rue d'Ulm - 75005 Paris - France  
`mickael.pechaud@ens.fr`  
<sup>2</sup> INSERM, U751, Marseille, France

**Abstract.** An important issue in electroencephalography (EEG) experiments is to measure accurately the three dimensional (3D) positions of the electrodes. We propose a system where these positions are automatically estimated from several images using computer vision techniques. Yet, only a set of undifferentiated points are recovered this way and remains the problem of labeling them, i.e. of finding which electrode corresponds to each point. This paper proposes a fast and robust solution to this latter problem based on combinatorial optimization. We design a specific energy that we minimize with a modified version of the Loopy Belief Propagation algorithm. Experiments on real data show that, with our method, a manual labeling of two or three electrodes only is sufficient to get the complete labeling of a 64 electrodes cap in less than 10 seconds.

## 1 Introduction

Electroencephalography (EEG) is a widely used method for both clinical and research purposes. Clinically, it is used e.g. to monitor and locate epilepsy, or to characterize neurological disorders such as sleeping or eating disorders and troubles related to multiple sclerosis. Its main advantages are its price compared to magnetoencephalography (MEG), and its very good time resolution compared e.g. to fMRI. Conventionally, EEG readings were directly used to investigate brain activity from the evolution of the topographies on the scalp. Nowadays, it is also possible to reconstruct the brain sources that gave rise to such measurements, solving a so-called inverse problem. To this purpose, it is necessary to find the electrode positions and to relate them to the head geometry recovered from an anatomic MRI. Current techniques to do so are slow, tedious, error prone (they require to acquire each of the electrodes in a given order with a device providing 3D coordinates[17]) and/or quite expensive (a specialized system of cameras is used to track and label the electrodes[23]). Our goal is to provide a cheap and easy system for electrode localization based on computer vision techniques.

In modern EEG systems, the electrodes (64, 128 or even 256) are organized on a cap that is placed on the head. Our system takes as inputs multiple pictures of the head wearing the cap from various positions. As a preliminary step,

electrodes are localized and their 3D positions are computed from the images by self-calibration (a technique that recovers the cameras’ positions from the image information [8]) and triangulation. These are standard techniques that can provide 3D point coordinates with a quite good accuracy. There remains the problem of electrode identification which labels each 3D position with the name of the corresponding electrode. Finding a solution to this last problem is the focus of this paper. Note, that a good labeling software can also improve current systems by removing acquisition constraints (such as the recording of the electrodes in a given order) and by providing better user interfaces.

We propose a method that recovers this labeling from just a few (two or three) manually annotated electrodes. The only prior is a reference, subject independent, 3D model of the cap. Our framework is based on combinatorial optimization (namely on an extension of the Loopy Belief Propagation algorithm[21]) and is robust to soft deformations of the cap caused both by sliding effects and by the variability in subjects’ head geometry.

## 2 Problem definition

The inputs of our method consist of:

- a template EEG cap model providing labeled electrodes, along with their 3D positions (in fact, as we will explain further, an important feature of our method is that only the distances between close electrodes are used).  $\mathcal{L}$  will denote the set of labels (e.g.  $\mathcal{L} = \{Fpz, Oz, \dots\}$ ), and  $C = \{C_l, l \in \mathcal{L}\}$  will be their corresponding 3D positions.  $C_l$  could be for example the average position of electrode  $l$  among a variety of prior measures. However, in our experiments, it was just estimated on one reference acquisition.
- the measured 3D positions of the electrodes to label, obtained by 3D reconstruction from images. We will denote by  $M = \{M_i, i \in [1..n]\}$ , these  $n$  3D points.

The output will be a labeling of the electrodes, i.e. a mapping  $\phi$  from  $[1..n]$  to  $\mathcal{L}$ . Note that  $n$  could be less than the total number  $|\mathcal{L}|$  of electrodes in cases where some electrodes of the cap are not used.

## 3 Motivation

In this section, we discuss other possible approaches for the electrode labeling problem. As it will be detailed in section 6, we have tried some of these methods without any success. This will motivate our energy-based combinatorial approach. A simple method could consist of a 3D registration step, followed by a nearest-neighbor labeling. Let  $T$  be a transformation that sends  $M$  into the spatial referential of  $C$ . A straight labeling could be:

$$\phi(i) = \arg \min_{l \in \mathcal{L}} d(C_l, T(M_i))$$

where  $d(A, B)$  denotes the Euclidean distance between points  $A$  and  $B$ . Actually, we first tested two direct ways of obtaining an affine transformation  $T$ :

- *moment-based affine registration*: in this case, we computed first and second order moments of the sets of points  $M$  and  $C$  and choose  $T$  as an affine transformation which superimposes these moments.
- *4 points manual registration*: here, we manually labeled 4 particular electrodes in  $M$  and took for  $T$  the affine transformation which exactly sends these 4 electrodes to the corresponding positions in  $C$ .

As explained in section 6, we observed that these two approaches give very bad average results. One could argue that this might be caused by the quality of the registration. A solution could be to use more optimal affine registration methods, like Iterative Closest Points[26, 3]. Yet, a close look at what caused bad labeling in our experiments, reveals that this would not improve the results : the main reasons are indeed that (i) the subject whose EEG has to be labeled does not have the same head measurements than the template, and moreover that (ii) the cap is a soft structure that shifts and twists from one experiment to another.

It is clear that only a non-rigid registration could send  $M$  close to  $C$ . The problem can be modeled in term of space deformation. For instance, a Thin-Plate Spline[5, 12] based algorithm follows this approach. Another framework is the deformable shape matching one : such methods rely on shape deformation and *intrinsic* shape properties[24] - rather than on deforming the ambient space - in order to make the shapes match. However, because of the topology of the electrodes on the cap, relations between points are also of importance. In that sense, our problem is close to the one investigated by Coughlan et al. [7, 1], which they solve recovering both deformations and soft correspondences between two shapes. Yet, in our case, we see two main differences : (i) labeling, rather than shape matching, is the key issue, and (ii) enforcing relational constraints between points are more important than regularizing deformations. For these reasons, we propose a method based on optimal labeling for which the only (soft) constraints are the distances between nearby points, without modeling any deformation. Our formulation also have the advantage of being parameter-free.

In the remaining of the article, we first state our model and the associated energy; we then discuss our choice for an energy minimization algorithm. Finally, we validate our method giving qualitative and quantitative results on real experiments.

## 4 Proposed framework

The complete pipeline of our system is depicted figure 1. As we already explained, we do not consider here the 3D reconstruction step, but only the labeling one. From the measured data  $M$ , we construct an undirected graph  $G = (V, E)$ , where  $V = [1..n]$  is the set of vertices and  $E$  a certain set of edges which codes the relations between nearby electrodes. As it will become clear in the following, the choice of  $E$  will tune the rigidity of the set of points  $M$ . Practically, the symmetric  $k$ -nearest neighbors or all the neighbors closer than a certain typical distance, are two valid choices. Given an edge  $e = (i, j) \in E$  for  $i \in V$  and  $j \in V$ , we denote by  $d_{ij} = d(M_i, M_j)$  the distance between points  $M_i$  and  $M_j$  in the measured data and by  $\tilde{d}_{ij} = d(C_{\phi(i)}, C_{\phi(j)})$  the reference distance between the

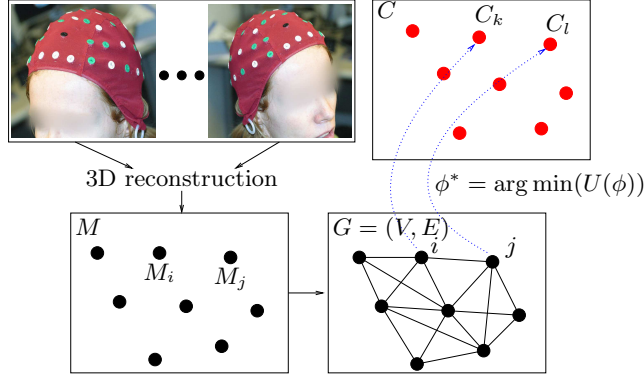


**Fig. 1.** Complete pipeline : we obtain 3D positions  $M$  (bottom left) by reconstruction from several (usually 6) pictures (top left). A graph  $G$  then is constructed from these positions (bottom right). Considering a template cap and associated positions  $C$  (top right), we label the measured electrodes by estimating  $\phi^* = \arg \min(U(\phi))$ . In this example,  $\phi(i) = k$ ,  $\phi(j) = l$ .

electrodes  $\phi(i)$  and  $\phi(j)$ . In order to preserve in a soft way the local structure of the cap, we propose to simply minimize the following energy:

$$U(\phi) = \sum_{(i,j) \in E} \rho(d_{ij}, \tilde{d}_{ij}) \quad (1)$$

where  $\rho$  is a cost-function which penalizes differences between the observed and template distances. Note that, whereas the global one-to-one character of  $\phi$  is not explicitly enforced by this model, the local rigidity-like constraints enforce it. Graph rigidity theory is a very complex domain (see for example [4] as an introduction), beyond the purpose of this article.

Following the classical framework of Markov Random Fields (MRF) [18, 2, 10], this can be rewritten as maximizing the following function:

$$P(\phi) = \exp(-U(\phi)) = \prod_{(i,j) \in E} \exp(-\rho(d_{ij}, \tilde{d}_{ij})) = \prod_{(i,j) \in E} \Psi_{i,j}(\phi(i), \phi(j)) \quad (2)$$

Normalizing  $P$  by dividing by the sum over all the possible mappings  $\phi$ , yields a *Gibbs distribution* over a MRF derived from graph  $G$  with  $\mathcal{L}$  as the set of possible labels each vertex. The problem is thus reduced to the classical case of finding a *Maximum A Posteriori* (MAP) configuration of a Gibbs distribution:

$$p(\phi) = \frac{1}{K} \prod_{i \in V} \psi_i(\phi(i)) \prod_{(i,j) \in E} \psi_{i,j}(\phi(i), \phi(j)) \quad (3)$$

where  $K$  is a normalizing constant.  $\psi_i$  represents some extra prior information which can be added to the model. We have  $\psi_i(\phi(i)) = 1$  if there is no prior

information over the labeling. However,  $\psi_i$  can be designed to take into account various priors. As explained in 6, we merely impose the label of some electrodes, but for example one could imagine using color information obtained from the pictures as a prior to the labeling.

## 5 Energy minimization

The problem of finding a MAP configuration of a Gibbs distribution being NP-complete [15], we cannot expect to get an algorithm that optimally solves every instance of the problem. Since the seminal work of Geman & Geman [10], who proposed an algorithm that warrants the probabilistic convergence toward the optimal solution – however with an unreasonable run-time – several methods have been investigated to maximize general distributions like (3). Among these, minimal-cut based methods (often referred to as *GraphCuts*), introduced in computer vision and image processing by [11], has received many attention (see [14, 6]). These methods can achieve global optimization for a restricted class of energies [13]. For more general energies, approximations were proposed [22]. As we experimented [19], these approximations fail to recover a correct labeling in our problem, which belongs to a class of multilabel problems that are not easily tackled by *GraphCuts*.

As a consequence, we opted for a completely different but widely spread algorithm, namely *Belief Propagation* (BP), and more precisely for its variant adapted to graphs: *Loopy Belief Propagation* (LBP). Please see [9] for a recent reference. Briefly, it consists in propagating information through the edges of the graph: each node  $i$  sends *messages* to its neighbors  $k$ , measuring the estimated label of  $k$  from its own point of view. Messages are passed between nodes iteratively until a convergence criterion is satisfied. This algorithm is neither guaranteed to converge nor to converge to an optimal solution. However, it behaves well in a large variety of early vision problems. Empirical and theoretical convergence of this family of methods were studied for instance in [20, 25].

Actually, we designed for this work an original and faster version of LBP. It is an improved version of LBP based on the idea of [16]. At the beginning of each iteration, it performs a label pruning at each node, which leads to a slight speed-up. However, unlike in [16], a pruned label can reappear in the next iterations, hence a non-greedy behavior of our algorithm.

Due to lack of place, we refer the reader to a detailed research report [19].

## 6 Experiments

We used 6 sets of 63 electrodes. Each set consists of 63 estimated three dimensional points, acquired on different subjects with the same EEG cap and manually labeled. To test our algorithm as extensively as possible, we ran the algorithm on each set, taking successively each of the other sets as a reference. We hence simulated 30 different pairs  $(M, C)$ . At least one electrode in  $M$  was manually labeled (see further).

$E$  was chosen the following way : we first estimated a typical neighbor distance by computing the maximum of the nearest neighbor distance for all electrodes in  $M$ , and then considered as belonging to  $E$ , every pair of distinct electrodes within less than three times this distance. In order to accelerate and enforce convergence, we used the three following technical tricks:

- we used our modified LBP algorithm[19]
- we added a classical momentum term ([20])
- denoting by  $V_f$  the subset of  $V$  of the manually labeled electrodes, we added the set of edges  $V_f \times V$  to  $E$ , allowing accurate information ( $V_f$  electrodes' labels being known exactly) to propagate quickly in the graph.

Although non indispensable, this led to a mean running time of less than 11s on a standard 3GHz PC and to a smaller number of non converging optimization.

The cost-function  $\rho$  was of the form  $\rho(x, y) = \frac{x}{y+\epsilon} + \frac{y}{x+\epsilon}$  where  $\epsilon$  is a small positive constant. We did not notice sensitivity with respect to this choice, as far as the following key conditions are fulfilled: (i) penalizing differences between  $x$  and  $y$  and (ii) penalizing small values of  $x$  or  $y$ . This latest condition enforces (yet does not warrant) a one-to-one mapping  $\phi$ .

Different experiments were carried out. First, the prior consisted in manually labeling electrodes  $Fpz$ ,  $Oz$ , and  $T8$ . In that case, our method recovers all the electrodes, which was, as expected, not at all the case with an affine registration+nearest neighbor approach (see figure 2). Actually, we observed that labeling ( $Oz, T8$ ) seems sufficient. Yet, without any further data, we do not consider that labeling two electrodes only is reliable. Figure 3 shows a result on a case where affine registration does not work and the final 3D reconstruction with our method.

To demonstrate the robustness of our algorithm, we also tested hundreds of other conditions, in which 1, 2 or 3 randomly chosen electrodes were "manually" labeled. Non-convergence was only observed for non reasonable choices of "manually" labeled electrodes: indeed, if they are chosen on the sagittal medium line, there is an undetermination due to the left-right symmetry of the cap. This does not occur when the electrodes are set by a human operator. The classification error rates are low (see figure 2 again) but not negligible. This makes us plead for a manual labeling of two or three fixed and easy to identify electrodes, e.g. ( $Fpz, Oz, T8$ ). Finally, we also successfully tested cases for which  $n < |\mathcal{L}|$ , i.e. when some electrodes are missing (details in [19]).

## 7 Discussion

Experiments show that our framework leads to fast, accurate and robust labeling on a variety of data sets. We consider providing on the WEB in a near future an complete pipeline including our algorithm - ranging from 3D reconstruction of electrodes to their labeling. Such a system would only require a standard digital camera and would imply minimal user interaction (manually labeling three electrodes).

Note that the flexibility of our  $MRF$  formulation allows different priors. We plan for instance to use the color of electrodes on the images as a further prior for

	<i>NC</i>	misclassified labels
Affine registration (moment based)	-	48.7%
Affine registration (4 manual points)	-	21.3%
Our method - ( <i>Fpz, Oz, T8</i> ) manually labeled	0%	0%
Our method - ( <i>Oz, T8</i> ) manually labeled	0%	0%
Our method - 3 random electrodes labeled	0%	0.03%
Our method - 2 random electrodes labeled	0.3%	0.2%
Our method - 1 random electrode labeled	4.2%	3.7%

**Fig. 2.** Classification errors. *NC* gives the percentage of instances of the problem for which our method did not converge. Misclassified labels percentages are estimated only when convergence occurs.

labeling. This could lead to a fully automated system, where no user interaction would be required.

## References

1. A.Rangarajan, J.M. Coughlan, and A.L. Yuille. A bayesian network framework for relational shape matching. In *9th IEEE ICCV*, pages 671–678, 2003.
2. J. Besag. Spatial interaction and the statistical analysis of lattice systems. *Journal Royal Statist. Soc.*, B-148:192–236, 1974.
3. P.J. Besl and N.D. McKay. A method for registration of 3-d shapes. *IEEE Trans. Pattern Anal. Mach. Intell.*, 14(2):239–256, 1992.
4. B.Hendrickson. Conditions for unique graph realizations. *SIAM J. Comput.*, 21(1):65–84, 1992.
5. F.L. Bookstein. Principal warps: Thin-plate splines and the decomposition of deformations. *IEEE Trans. PAMI*, 11(6):567–585, 1989.
6. Y. Boykov, O. Veksler, and R. Zabih. Markov random fields with efficient approximations. In *CVPR '98*, page 648, Washington, DC, USA, 1998. IEEE.
7. J.M. Coughlan and S.J. Ferreira. Finding deformable shapes using loopy belief propagation. In *7th ECCV*, pages 453–468, 2002.
8. O. Faugeras, Q.T. Luong, and T. Papadopoulos. *The Geometry of Multiple Images*. MIT Press, 2001.
9. P. Felzenszwalb and D. Huttenlocher. Efficient belief propagation for early vision, 2004.
10. S. Geman and D. Geman. Stochastic relaxation, gibbs distributions, and the bayesian restoration of images. *IEEE Trans. PAMI*, 6(6):721–741, Nov. 1984.
11. D.M. Greig, B.T. Porteous, and A.H. Seheult. Exact maximum a posteriori estimation for binary images. *J. R. Statist. Soc. B*, 51:271–279, 1989.
12. H.Chui and A. Rangarajan. A new algorithm for non-rigid point matching. In *CVPR*, pages 2044–2051, 2000.
13. H. Ishikawa. Exact optimization for markov random fields with convex priors, 2003.
14. H. Ishikawa and D. Geiger. Mapping image restoration to a graph problem, 1999.
15. V. Kolmogorov and R. Zabih. What energy functions can be minimized via graph cuts? In *ECCV (3)*, pages 65–81, 2002.

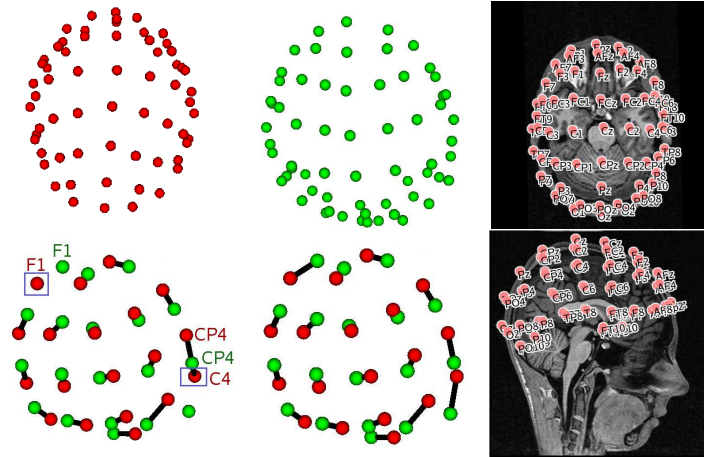


**Fig. 3.** A sample result.  $M$  is in red and  $C$  in green. Top left: 63 estimated 3D electrodes positions. Top center: reference. Bottom left: subset of a labeling with the moment based algorithm;  $C4$  is wrongly labeled  $CP4$ , and  $F1$  is labeled  $F3$  (not shown). Bottom center: a subset of correct correspondences retrieved by our algorithm. Top and bottom right: full labeling retrieved by our algorithm, superimposed with anatomical MRI

16. N. Komodakis and G.Tziritas. Image completion using global optimization. In *CVPR '06*, Washington, DC, USA, 2006. IEEE Computer Society.
17. D. Kozinska and K. Nowinski. Automatic alignment of scalp electrode positions with head mri volume and its evaluation. In *Engineering in Medicine and Biology, BMES/EMBS Conference*, Atlanta, Oct 1999.
18. P. Lévy. Chaînes doubles de markov et fonctions aléatoires de deux variables. *C.R.Académie des sciences*, 226:53–55, 1948.
19. M.Pechaud, R.Keriven, and T.Papadopoulo. Combinatorial optimization for electrode labeling of EEG caps. Technical Report 07-32, CERTIS, July 2007.
20. K.P. Murphy, Y. Weiss, and M.I. Jordan. Loopy belief propagation for approximate inference: An empirical study. In *Fifteenth Conference on Uncertainty in Artificial Intelligence*, pages 467–475, 1999.
21. J. Pearl. *Probabilistic Reasoning in Intelligent Systems: Networks of Plausible Inference*. Morgan Kaufmann Publishers, Inc., 1988.
22. A. Raj and R. Zabih. A graph cut algorithm for generalized image deconvolution. In *ICCV '05*, pages 1048–1054, Washington, DC, USA, 2005. IEEE.
23. G. S. Russell, K. J. Eriksen, P. Poolman, P. Luu, and D. M. Tucker. Geodesic photogrammetry for localizing sensor positions in dense-array eeg. *Clinical Neurophysiology*, 116:1130–1140, 2005 (see also [http://www.egi.com/c\\_gps.html](http://www.egi.com/c_gps.html)).
24. T.B. Sebastian, P.N. Klein, and B.B. Kimia. Alignment-based recognition of shape outlines. In *4th International Workshop on Visual Form*, pages 606–618, 2001.
25. Y. Weiss and D. Freeman. On the optimality of solutions of the max-product belief-propagation algorithm in arbitrary graphs. *IEEETIT*, 47, 2001.
26. Z. Zhang. iterative point matching for registration of free-form curves. Technical Report RR-1658, INRIA, 1992.